International Journal of Heat and Mass Transfer 136 (2019) 962–971

Contents lists available at ScienceDirect

International Journal of Heat and Mass Transfer

journal homepage: www.elsevier.com/locate/ijhmt

Multi-component droplet evaporation model incorporating the effects of non-ideality and thermal radiation

Bin Fang, Longfei Chen *, Guangze Li, Lei Wang

School of Energy and Power Engineering, Beihang University, Beijing 100191, China

ARTICLE INFO

Article history:
Received 1 September 2018
Received in revised form 8 February 2019
Accepted 8 March 2019
Available online 18 March 2019

Keywords:
Non-ideal liquid
Activity coefficients
Thermal radiation
Droplet evaporation

ABSTRACT

Currently, sophisticated fuel formulation and high temperature combustion in gas turbine and internal combustion engines make it important to investigate the effects of mixture non-ideality and radiation absorption on fuel droplet evaporation. In this study, an improved evaporation model by considering activity coefficients (AC) and external thermal radiation was established to simulate the evaporation process of multi-component non-ideal fuel droplets, and droplet suspension experiment was performed to validate the proposed model. It was found that the accuracy of simulated results was enhanced by considering activity coefficients and radiation absorption, and both effects were dependent on ambient temperature. The effect of activity coefficient was significant at low temperature (503 K), under which the droplet evaporation rate in the initial period was obviously faster than that at later stage. Consequently, the droplet lifetime decreased by about 8% at low temperature when activity coefficient was taken into consideration. At high temperature (703 K), however, the effect of activity coefficient or non-ideality on the droplet evaporation rate turned out to be insignificant. The radiation had a strong influence on evaporation at high temperature with the droplet lifetime decreasing 48% when ambient temperature increased from 503 K to 703 K. There seemed to be a critical diameter, under which the effect of radiation became negligible. It is also demonstrated that the component concentration gradients existed inside the non-ideal droplets in the initial period because of relatively low mass diffusion rate. As time elapsed, the gradients gradually disappeared due to the fact the components with large activity coefficient nearly completely evaporated.

1. Introduction

Droplet evaporation is an important process for liquid fuel combustion systems such as internal combustion engines and gas turbine engines, in which the liquid fuel is atomized into fine droplets in the combustion chamber, followed by droplet evaporation in high temperature environment. The droplet evaporation process normally involves the heat and mass transfer of a mixture of various compounds [1], and it is thus important to accurately predict the evaporation process of multi-component fuel droplets in high temperature environment for spray combustion design and analysis [2].

Law et al. [3] proposed a multi-component droplet evaporation model under the assumption that the component concentration and temperature inside droplets were spatially uniform but varied with time. The model was referred to as the infinite diffusion model. Based on the assumption of this model, the multi-component droplet evaporation process is similar to batch distillation, and the volatile components are continuously brought to the droplet surface for preferred evaporation. Landis and Mills [4] studied the evaporation characteristics of three-component fuel droplets in stagnant environments and developed another model. They considered that both temperature and component concentration varied spatially and temporally within droplets. The governing equations were derived to describe the gradients of temperature and component concentration inside droplets. Megaridis and Sirignano [5] conducted a further research based on the diffusion control model, which took into account of the temperature dependence of liquid-phase density and heat capacity. The results demonstrated that convection influenced liquid density via temperature variation, yet liquid heat capacity was fairly constant.

For multi-component fuels, the interactions between identical molecules and those between dissimilar molecules could be significantly different. Especially for non-ideal mixtures, polar molecules and non-polar molecules exist simultaneously, and the attraction between non-polar molecules is London dispersion force, which is less than other types of intermolecular forces, while the attrac-

* Corresponding author.
E-mail address: chenlongfei@buaa.edu.cn (L. Chen).

https://doi.org/10.1016/j.ijheatmasstransfer.2019.03.051
0017-9310/

Nomenclature

$\dot{m}$	droplet evaporation rate, g/s
r_s	droplet transient diameter, mm
ρ	average density of gas phase, kg/m^3
$D_{i,g}$	diffusion coefficient of gas, m^2/s
$D_{i,L}$	diffusion coefficient of liquid, m^2/s
Sh	Sherwood number
Sh'	modified Sherwood number
Nu	Nusselt number
Nu'	modified Nusselt number
$c_{p,iv}$	constant pressure specific heat capacity, J/(kg·K)
$k_{i,g}$	thermal conductivity of gas, W/(m·K)
$B_{M,i}$	mass transfer number
$B_{T,i}$	heat transfer number
$Y_{i,VS}$	mass fraction of vapor at gas-liquid interface
$Y_{i,V\infty}$	mass fraction of vapor at infinity of droplet
T_0	temperature in the center of droplet, K
T_∞	temperature at infinity of droplet, K
L_{eff}	effective enthalpy of evaporation, kJ/kg
L	latent heat of vaporization, kJ/kg
$X_{F,i}$	mass fraction in the liquid phase
γ_i^C	combination part
γ_i^R	independent part
y_i	mole fraction in the vapor
ω_i	mole fraction in droplet
ρ_L	liquid density, kg/m^3
λ_L	thermal conductivity of liquid, W/(m·K)
c_{pL}	specific heat capacity of liquid, J/(kg·K)
p_{vpi}	saturated vapor pressure, Pa
$P(r)$	power in unit volume inside droplet due to external radiation
Δr	length of each calculation segment
Q_a	efficiency factor of absorption
$B_\lambda(T_g)$	Planck function
T_g	gas temperature, K
Q_{rad}	thermal radiation absorption of droplet, J
k_λ	index of absorption
α_λ	absorption coefficient

Subscript

i	component$i$

Abbreviations

AC	activity coefficients
w/o	without
DL	droplet lifetime

tion between polar molecules is dipole-dipole force, which is relatively strong [6–8]. Therefore, multi-component non-ideal droplets normally exhibit complicated evaporation behaviors compared to single component or ideal droplets [9–11]. This complexity is presented in two aspects: First, the composition and temperature of droplets and their adjacent vapor vary continuously over time during the evaporation progress; Second, there exist composition and temperature gradients within the droplet which are also subject to transient evolution.

For simulating non-ideal fuel evaporation, previous models incorporating component activity coefficient have been proposed to reflect the non-ideality of multi-component droplets. The component activity coefficient acts as a metric quantifying the extent to which several laws of physical chemistry (such as Raoult's law) for ideal solutions deviate from realistic non-ideal mixtures [12,13]. Thus the introduction of component activity coefficient could be imperative to account for the effect of non-ideality on the evaporation rate of each component. However, the activity coefficient for each component was assumed to be unity in the majority of previous studies [14–16], which means that the deviation between ideal mixture and real mixture was assumed to be nil. Only few studies essentially took the activity coefficients into account, for example, Brenn et al. [17] proposed a multi-component droplet evaporation model which treated the liquid phase as a thermodynamically real fluid, and the universal functional activity coefficient (UNIFAC) method which was based on the group contribution was used to calculate the component activity coefficients. The results indicated that the model can basically capture the physico-chemical phenomena in multi-component liquid droplet evaporation. Al-Esawi et al. [18] designed a discrete component model and took into account the liquid non-ideality with UNIFAC method to investigate the heating and evaporation of ethanol/gasoline fuel blend droplets. The results showed that the model without considering non-ideality led to up to 5.7% error in estimated droplet lifetime for ethanol/gasoline blends, compared to the predictions using the UNIFAC approach. Diddens et al. [19] developed a mathematical model for the drying of sessile droplets of binary mixtures, in which the activity coefficients were accounted for non-ideal interactions of the species. The activity coefficients were calculated by the activity coefficient model Aerosol Inorganic-Organic Mixtures Functional groups Activity Coefficients (AIOMFAC). The AIOMFAC combined a Pitzer-like electrolyte solution model with a UNIFAC-based group-contribution approach and explicitly accounted for interactions between organic functional groups and inorganic ions [20]. The results demonstrated a good agreement with experimental findings.

Fuel droplets evaporate in combustors due to continuous heat absorption. Except for heat conduction and heat convection, fuel droplets also absorb heat via thermal radiation from high temperature environment. The thermal radiation energy is primarily determined by the temperature of radiation sources and the absorption of the fuel. Due to the complexity of thermal radiation calculations, most of previous studies on droplet evaporation ignored the heat absorption via thermal radiation [21]. As the internal temperature of most combustors are very high, the heat droplets absorbed from high temperature environment via thermal radiation may not be safely neglected, thus developing an advanced evaporation model by considering thermal radiation is desirable. Abramzon et al. [22] designed a model to investigate the vaporization behavior of *n*-decane and diesel droplets under high ambient temperature conditions by considering radiation absorption. It was found that thermal radiation absorption in diesel fuel was generally stronger than in *n*-decane, which may be attributed to the different molecular bonds presented in the different fuels. Tseng et al. [23] developed a mathematical model incorporating radiation for the unsteady evaporation of a water droplet. The radiation absorption was calculated by a radiative transfer model based on geometrical optics theory. The results demonstrated that the absorption of radiation significantly affected the lifetime of the droplet. The lack of radiation consideration led to the underestimation of the water evaporation rate especially for droplets with a diameter of greater than 500 mm. Dombrovsky and Sazhin [24] proposed a model of calculating the distribution of thermal radiation inside the droplet by improving the MDP_0 approximation model [25] which was a preliminary model of con-

sidering radiation power absorption. The model assumed that the external radiation to droplet was symmetrical, and the results showed that the distribution of radiation power absorption within droplet was asymmetrical. Long et al. [26] used this model to simulate droplet evaporation by taking into account of the thermal radiation. Their results indicated that the simulated data were closer to the experimental results when considering external thermal radiation in a high temperature environment. They also established a critical diameter criterion at a certain temperature, which could be used to determine whether external radiation needs to be considered.

Previous studies on radiation all used single component or quasi-ideal binary mixture test fuels, which obey Raoult's law and thus experienced steady evaporation process. To authors' knowledge, there is no literature reporting the radiation effects on the transient evaporation process for non-ideal multi-component fuel droplets. It would be desirable to couple the thermal radiation distribution inside droplets with the transient calculation of component distribution inside droplets for more practical and realistic biofuels which are normally highly non-ideal. In this study, a multi-component droplet evaporation model incorporating thermal radiation was proposed, which explored the combined effects of fuel non-ideality and thermal radiation adsorption on the transient evaporation process. The activity coefficients of the components in the mixed solution were calculated via UNIFAC method to quantify the non-ideality of blended fuels. The radiation power absorption was considered by coupling a radiation model with the droplet heat and mass transfer governing equations. As *n*-decane, toluene and butanol are often selected as surrogate fuel constituents for both gas turbine and internal combustion engine applications, the blends of these components were used as test fuels in this study. The proposed model was validated by suspension droplet evaporation experiments, and the effects of fuel non-ideality and thermal radiation on the evaporation rate were demonstrated.

2. Model description and experiment

2.1. Multi-component droplet evaporation model

In the process of droplet evaporation, the composition and temperature of non-ideal droplets vary over time, and the differences between individual component in terms of mass diffusion and volatility are key factors affecting the evaporation characteristics of multi-component droplets. To incorporate these factors, the activity coefficients calculation was coupled with the multi-component droplet evaporation model to predict transient evaporation process. In addition, a thermal radiation model was used to reflect the influence of high temperature environment around the droplet.

Fig. 1 is a schematic diagram of a droplet evaporation model. The model is based on the following assumptions: (1) the droplet always maintains spherical symmetry; (2) the gas dissolution into droplets is ignored; (3) external radiation to the droplet is assumed to be spherically symmetrical; (4) the droplet is regarded to be semi-transparent.

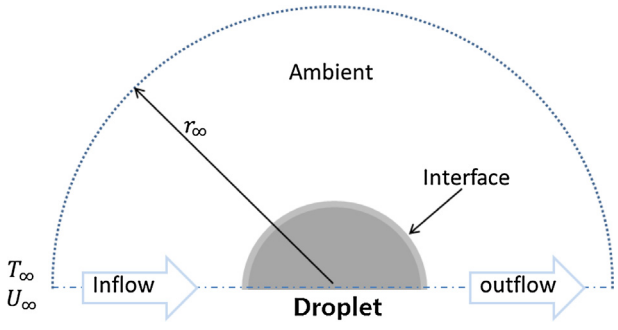

Fig. 1. Schematic diagram of droplet evaporation model.

2.1.1. Governing equations of heat and mass transfer

The evaporation rate of a multi-component droplet is the sum of the evaporation rate of individual component, which can be calculated from Eqs. (1) and (2) [27].

$$\dot{m} = \sum_{i=1}^{n} \dot{m}_i = 2\pi \sum_{i=1}^{n} r_s \bar{\rho} D_{i,g} Sh' \ln(1 + B_{M,i}) \tag{1}$$

$$\dot{m} = \sum_{i=1}^{n} \dot{m}_i = 2\pi \sum_{i=1}^{n} r_s k_{i,g} Nu' \ln(1 + B_{T,i})/c_{p,iv} \tag{2}$$

where $\dot{m}_i$ represents the evaporation rate of the component i; r_s is the droplet transient diameter; $\bar{\rho}$ is the average density of gas phase; $D_{i,g}$ is the diffusion coefficient of component i in the gas phase, $D_{i,g}$ can be calculated by the method of Fuller et al., which can be found in the book of Poling et al. [28]; $k_{i,g}$ is the gas thermal conductivity of component$i$; Sh is the Sherwood number; Nu is the Nusselt number; $c_{p,iv}$ is the gas constant pressure specific heat capacity of component i; B_M is mass transfer number; B_T is heat transfer number. The mass and heat transport numbers are calculated using the following formulas respectively:

$$B_{M,i} = \frac{Y_{i,VS} - Y_{i,V\infty}}{1 - Y_{i,VS}} \tag{3}$$

$$B_{T,i} = \frac{c_{p,iv}(T_\infty - T_0)}{L_{eff}} \tag{4}$$

where $Y_{i,VS}$ is the mass fraction of the vapor of the component i at the gas-liquid interface; $Y_{i,V\infty}$ is the mass fraction of the vapor of the component i at infinity; L_{eff} is the effective enthalpy of evaporation, and its expression is as follows:

$$L_{eff} = L + \frac{(4\pi r_s^2 \lambda_L \frac{dT}{dr}|_{S,L} + Q_{rad})}{\dot{m}} \tag{5}$$

$$L = \sum_{i=1}^{N} X_{F,i} L_i \tag{6}$$

where L represents the latent heat of vaporization of the mixed fuel; $X_{F,i}$represents the mass fraction of component i in the liquid phase; L_i represents the latent heat of vaporization of component$i$; Q_{rad} represents heat absorption of droplet due to external thermal radiation, and the method of calculating Q_{rad} will be discussed in Section 2.1.2. In reality, the droplet is not stationary, which involves the effect of forced convection on the evaporation rate. It is necessary to correct the evaporation rate by Sh number, and the calculation method ofSh number under convection condition is presented as follows [29]:

$$Sh_0 = 2 + f(Re, Sc) \tag{7}$$

$$f = \begin{cases} (1 + ReSc)^{1/3} - 1, & Re < 1 \\ (1 + ReSc)^{1/3} Re^{0.077} - 1, & Re > 1 \end{cases} \tag{8}$$

$$Sh' = 2 + \frac{(Sh_0 - 2)B_M}{(1 + B_M)^{0.7} \ln(1 + B_M)} \tag{9}$$

The calculation of Nusselt number is as follows:

$$Nu_0 = 2 + f(Re, Pr) \tag{10}$$

$$f = \begin{cases} (1 + Re \cdot Pr)^{1/3} - 1, & Re < 1 \\ (1 + Re \cdot Pr)^{1/3} Re^{0.077} - 1, & Re > 1 \end{cases} \tag{11}$$

$$Nu' = 2 + \frac{(Nu_0 - 2)B_T}{(1+B_T)^{0.7}\ln(1+B_T)} \tag{12}$$

The Clausius-Clapeyron equation and Raoult's law can be used to calculate the mole fraction of the vapor at the droplet surface under specific pressure and temperature conditions, and it is normally assumed that the surface of the droplet is in the equilibrium state of gas-liquid phase. However, Raoult's law is no longer applicable for non-ideal solutions. It is necessary to introduce the activity coefficients to correct the evaporation rate of each component. The corrected Raoult's law is:

$$y_i p = \gamma_i x_i p_{vpi} \tag{13}$$

where y_i is the mole fraction of component$i$ in the vapor; p is the gas pressure; γ_i is the activity coefficient of component$i$; x_i is the mole fraction of component i within the droplet; p_{vpi} is the saturated vapor pressure of component i in the absence of other components.

Activity coefficient γ_i is obtained using the UNIFAC method. The activity coefficient is divided into two parts, one part γ_i^C emphasizes on the size and shape impact on the activity coefficient and the other part γ_i^R emphasizes on the interaction between the functional groups within the molecule.

$$\ln\gamma_i = \ln\gamma_i^C + \ln\gamma_i^R \tag{14}$$

The specific calculation of the activity coefficient by UNIFAC method can be obtained from the literacy of Govindaraju et al. [30].

As the evaporation process of multi-component droplets is accompanied by mass diffusion process within droplets, there exist temperature and concentration gradient inside droplet, which could be taken into account by using diffusion control model. The governing equations of heat and mass transfer of multi-component droplets under spherical coordinates are as follows:

$$\frac{\partial T}{\partial t} = \theta\left(\frac{\partial^2 T}{\partial r^2} + \frac{2}{r}\frac{\partial T}{\partial r}\right) + \frac{P(r)}{\rho_L c_{pL}} \tag{15}$$

$$\frac{\partial X_i}{\partial t} = D_{i,L}\left(\frac{\partial^2 X_i}{\partial r^2} + \frac{2}{r}\frac{\partial X_i}{\partial r}\right) \tag{16}$$

where the thermal diffusivity is $\theta = \lambda_L/\rho_L c_{pL}$; $\lambda_L$represents the thermal conductivity of droplets; ρ_L represents the density of droplets; c_{pL} represents the specific heat capacity of the droplet; $P(r)$ is the power in unit volume inside the droplet due to external radiation, and it will be introduced in detail in the following section; $X_{i,L}$ is mass fraction of component i in the droplet; $D_{i,L}$ is diffusion coefficient of component i in the multi-component droplets. And $D_{i,L}$ is also calculated by the method described in the book of Poling et al. [28] The boundary conditions are as follows:

At droplet center r = 0: $\frac{\partial T}{\partial r}|_0 = 0$; $\frac{\partial X_i}{\partial r}|_0 = 0$

At droplet surface $r = r_s$: $4\pi r_s^2 \lambda \frac{\partial T}{\partial r}|_S = \dot{m}(L_{eff} - L) - Q_{rad}$; $\frac{\partial X_i}{\partial r}|_S = \frac{\dot{m}(X_i - \varepsilon_i)}{4\pi\rho_L D_{i,L} r_s^2}$

ε_i is the ratio of the evaporation rate of component i to the total evaporation rate and could be expressed by [31]:

$$\varepsilon_i = \frac{Y_{i,VS}(1+B_M)}{B_M} \tag{17}$$

The aforementioned governing equations can be solved by the finite difference method in Crank-Nicolson format. The radius of the droplet is divided into N parts with the length of each segment being Δr. To ensure calculation convergence, the time step was set as $\Delta t \le (\Delta r)^2/2\theta$.

2.1.2. Thermal radiation absorption

Compared with previous radiation studies on droplet evaporation for single-component or ideal mixture fuels, we incorporated the transient component distributions within droplets into the heat radiation calculation, which would be more realistic for non-ideal mixture such as biofuels. It is assumed that the external thermal radiation is spherically symmetrical. The following model is used to calculate the power in unit volume inside the droplet due to the external radiation [24]:

$$P(r) = \frac{3\pi}{r_s}\int_{\lambda_1}^{\lambda_2} w(r_n,\lambda) Q_a B_\lambda(T_g) d\lambda \tag{18}$$

where λ_1 and λ_2 are used to define the main spectrum range in which droplet absorbs heat via thermal radiation; $w(r_n,\lambda)$ is the normalized spectral power of radiation per unit volume absorbed inside the droplet; Q_a is the efficiency factor of absorption; $B_\lambda(T_g)$ is the Planck function; T_g is gas temperature. The determination of these terms can be found elsewhere in literature [32]. Based on the calculated $P(r)$, the total heat absorbed by the entire droplet via external radiation is:

$$Q_{rad} = \int_0^{r_s} 4\pi r^2 P(r) dr \tag{19}$$

It is well established that different materials exhibit different selectivity, in other words, different components primarily absorb thermal radiation power in different spectrum range. Thus it is indispensable to obtain the absorption coefficient in the specific spectrum range prior to calculating $P(r)$. The absorption spectrum of n-decane can be found from [33], and those for butanol and toluene can be obtained elsewhere [34,35]. The spectrum describes the variation of index of absorption k_λ over wavelength λ. The relationship between the absorption coefficient α_λ and the index of absorption k_λ is as follows [32]:

$$\alpha_\lambda = \frac{4\pi k_\lambda}{\lambda} \tag{20}$$

In order to calculate the radiation absorption more conveniently, the absorption spectrums of n-decane, butanol and toluene were approximated via multi-stage fitting algorithm. Taking n-decane as an example, the determination of its absorption coefficient is illustrated in Fig. 2.

The approximation of the index of absorption k for n-decane is in the form of $k = 10^{\psi}$, where the expressions of ψ in different range are listed in Table 1.

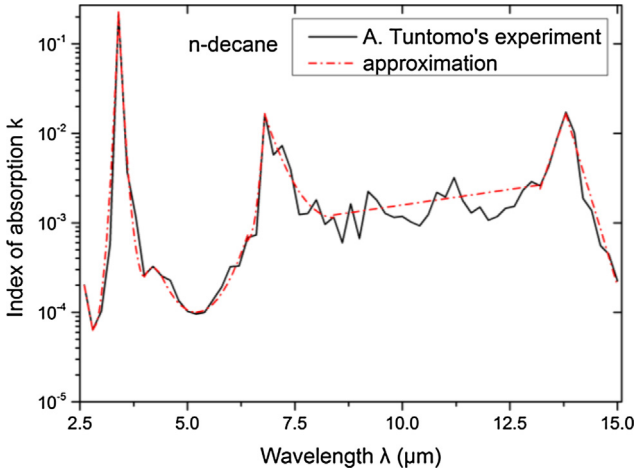

Fig. 2. The absorption spectrum of n-decane.

Table 1
The list of expressions of ψ in multi-stage of absorption wavelength of *n*-decane.

Number	Wavelength range λ (μm)	Expressions of ψ
(1)	$2.6 \le \lambda \le 2.8$	$\psi = -2.5\lambda + 2.8$
(2)	$2.8 \le \lambda \le 4.2$	$\psi = 9.9(\lambda - 2.8)^2 - 4.2$
(3)	$3.4 \le \lambda \le 4$	$\psi = 8.2(\lambda - 4)^2 - 3.6$
(4)	$4.0 \le \lambda \le 4.4$	$\psi = -2.6(\lambda - 4.2)^2 - 3.5$
(5)	$4.4 \le \lambda \le 5.2$	$\psi = 0.63(\lambda - 5.2)^2 - 4$
(6)	$5.2 \le \lambda \le 6.4$	$\psi = 0.6(\lambda - 5.2)^2 - 4$
(7)	$6.4 \le \lambda \le 6.8$	$\psi = 8.9(\lambda - 6.4)^2 - 3.2$
(8)	$6.8 \le \lambda \le 8.4$	$\psi = 0.45(\lambda - 8.4)^2 - 2.94$
(9)	$8.4 \le \lambda \le 13.2$	$\psi = 0.7\lambda - 3.5$
(10)	$13.2 \le \lambda \le 13.8$	$\psi = 1.4\lambda - 21.1$
(11)	$13.8 \le \lambda \le 15$	$\psi = -1.6\lambda + 20.3$

For the calculation of the heat absorption via radiation of the mixed fuel droplets, the proportional superposition method is adopted as follows:

$$P(r)_t = \sum_{i=1}^{n} \omega_i P(r)_i \tag{21}$$

where ω_i is the mole fraction of component *i* in the position r along the radius of the droplet; Since ω_i is a transient value, the heat absorbed via radiation also changes temporally and spatially; $P(r)_i$ is the power in unit volume inside the droplet due to the external radiation when the droplet consists of pure component *i*.

2.2. Experimental

To verify the accuracy of the proposed model, a suspended droplet evaporation experiment was conducted. The droplet was suspended in a furnace by thermocouple wire. The thermocouple wire was used not only to measure gas temperature inside the furnace but also to be the size reference (0.1 mm). A backlit was located in the opposite side of a high speed camera. The high speed camera took a series of images of the droplet throughout the evaporation process. The initial droplet diameter was in the range of 1.0 mm to 1.2 mm, and the initial droplet temperature was at room temperature (about 298 K). Two different test fuels were used: a mixture of 80% vol. *n*-decane, 15% vol. toluene, 5% vol. butanol, and a mixture of 70% vol. *n*-decane, 15% vol. toluene, 15% vol. butanol. The evaporation experiment for both fuel droplets were conducted at 503 K and 703 K. The initial droplet diameter was kept largely constant, and the experiment under each condition was repeated for four times and the average values were taken for analysis.

The droplet diameter was derived from the images using a MATLAB-based program. Due to gravity and surface tension, the suspended droplet was in ellipsoid shape which was clearly showed in Fig. 3(a). It was assumed that the suspended droplet was a standard spheroid which means that the cross-section of the droplet that is vertical to the long axis is a circle. The original photos were firstly converted to binary picture which was presented in Fig. 3(b). The contour of droplet was then captured and the long axis and short axis were obtained as 2a and 2b respectively. Thus the volume of the droplet could be approximated by the following equation:

$$v = \frac{4\pi ab^2}{3} \tag{22}$$

The equivalent diameter of spherical droplet with equal volume could be obtained as follows:

$$\frac{4\pi ab^2}{3} = \frac{4\pi(\frac{d}{2})^3}{3} \tag{23}$$

It could be simplified as:

$$d = 2\sqrt[3]{ab^2} \tag{24}$$

3. Results analysis and discussion

The droplet diameter changing rate is an important metric for characterizing droplet evaporation, and Godsave et al. [36] proposed a quasi-steady-state model or D^2 law, which specifies that the attenuation of droplet squared diameter over the evaporation time is linear. However, this classical model lacks of the consideration of non-ideality effect of multi-component droplets and the radiation effect on the evaporation, hence the linear D^2 law may not be valid for simulating the evaporation of real non-ideal droplets whose composition varies over time.

3.1. The effects of non-ideality on droplet evaporation

Figs. 4 and 5 exhibit the evaporation process of the two test droplets and the simulated results derived from the models with and without (w/o) considering activity coefficients. The curves with considering activity coefficients were generally closer to the exper-

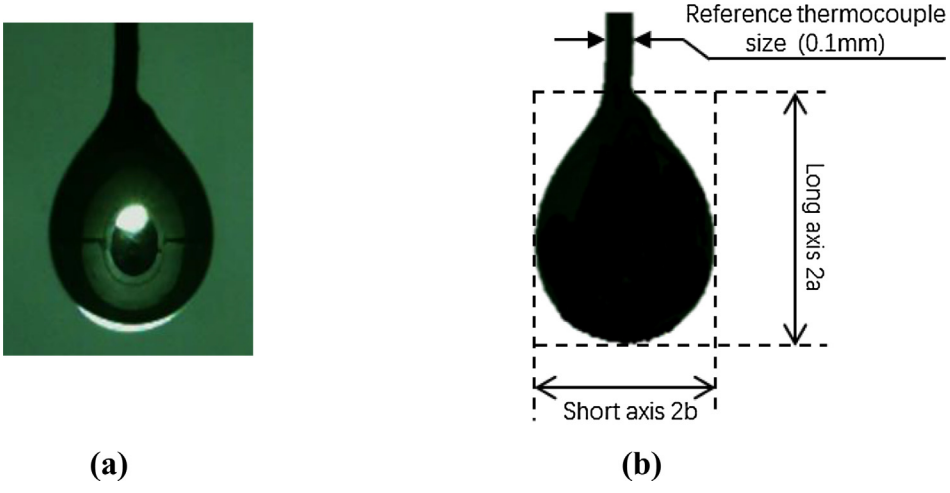

Fig. 3. Typical droplet image in the evaporation process: (a) the original droplet image captured by the high speed camera, (b) the binary image converted from original image.

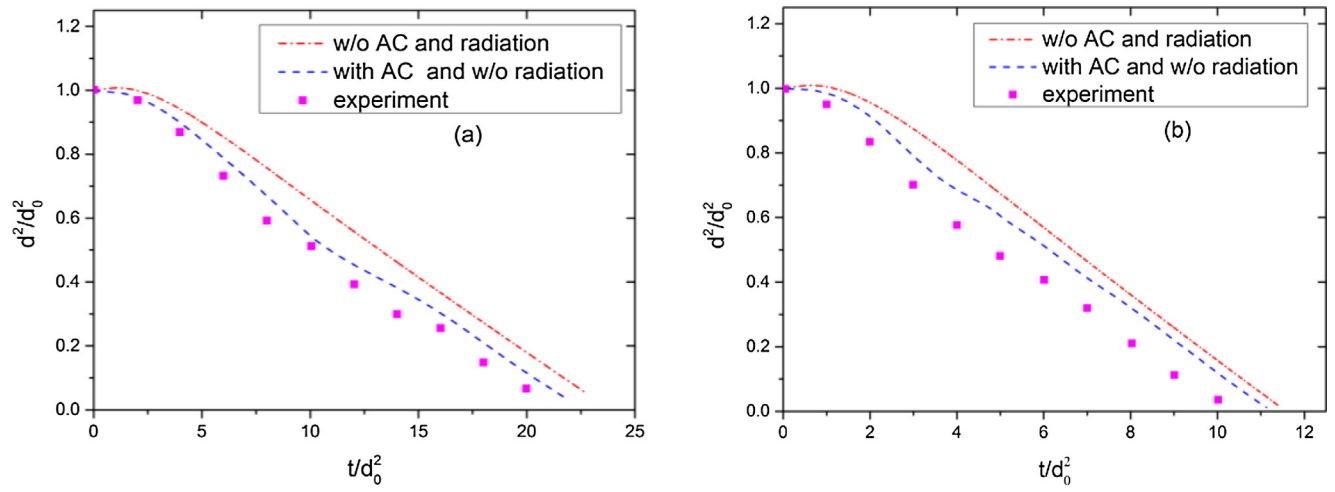

Fig. 4. Squared diameter versus time for droplets of 80% vol. *n*-decane, 15% vol. toluene, and 5% vol. butanol at two different gas temperatures (a) 503 K, (b) 703 K and predicted results with and without considering activity coefficients.

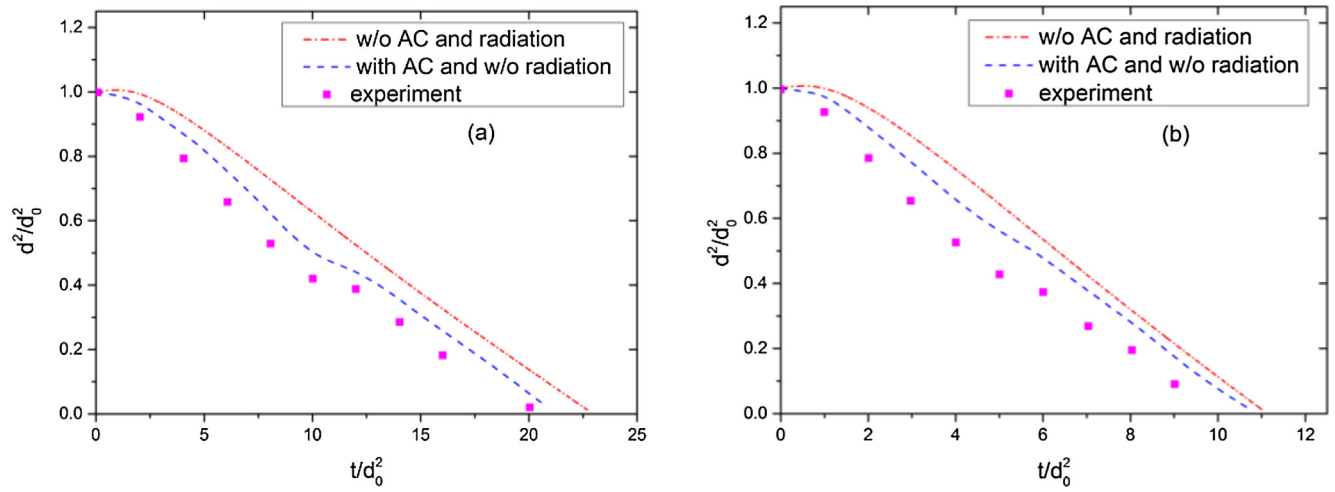

Fig. 5. Squared diameter versus time for droplets of 70% vol. *n*-decane, 15% vol. toluene, and 15% vol. butanol at two different gas temperatures (a) 503 K, (b) 703 K and predicted results with and without considering activity coefficients.

imental data compared to those without considering non-ideality. Unlike the curve of ideal assumption, the non-unity activity coefficient caused a marked deviation from D^2 law, in other words, the slope of the curve varied over evaporation process. This was presumably caused by the fact that the droplet composition changed unsteadily over time for non-ideal simulation. Due to the molecular polarity differences, butanol has much stronger polarity than *n*-decane, thus it has larger activity coefficient than *n*-decane. The activity coefficient of toluene (5.2–6.3) lies between butanol (8.8–10.2) and *n*-decane (1.3–2.5). The higher the activity coefficient, the faster the evaporation occurs. This non-ideality would result in the varying droplet composition during evaporation, which will in turn lead to unsteady change in component activity coefficient, droplet density, thermal conductivity and Spalding mass transfer number among others. In this case, the attenuation rate of droplet diameter varied unsteadily over time, so did the evaporation rate. It is worth noting that there was an initial 'plateau' region for ideal curve which was probably caused by thermal expansion effect during the droplet preheating period [37,38]. Yet for the situation with considering the activity coefficients, the initial preheating period became shorter. The main reason might be that the butanol with higher activity coefficient evaporated relatively fast even at low temperature.

Despite the discrepancy caused by non-ideality consideration, the evolution of the droplet squared diameter over time was still broadly in line with D^2 law. The mass transfer number $B_{M,i}$ is a term in the Eq. (1) which influences the evaporation rate. The mass transfer number $B_{M,i}$ is related to vapor mass fraction of component *i* at the droplet interface $Y_{i,VS}$ according to Eq. (3). And $Y_{i,VS}$ is further related to the activity coefficient γ_i according to Eq. (10). Under the test conditions, the contribution by activity coefficient γ_i was relatively insignificant compared to the *Sh* number which increased with Reynolds (*Re*) number [39].

By comparing Figs. 4(a), (b), 5(a) and (b), it could be found that the influence of activity coefficients on evaporation at low gas temperature was more conspicuous than that at high temperature. The *Re* and *Sh* number were relatively large at high temperature, and droplet evaporation rate was faster at high temperature, yet the effect of activity coefficient became less significant in heat transfer dominated evaporation process [39,40]. In addition, there seemed to be only a minor difference of droplet lifetime between the cases with and without considering activity coefficients. This may attri-

bute to the fact that both fuels had the highest volume fraction of *n*-decane and thus the interaction parameters calculated by the UNIFAC model for the different test fuels were not significantly different.

3.2. The effects of heat radiation on droplet evaporation

Figs. 6 and 7 show the evaporation process of the two test droplets and the simulated results derived from the models with and without considering radiation. In general, the results of considering radiation were closer to experimental data compared with the non-radiation calculation. But for the results with considering radiation, the slope of the curves of the droplet squared diameter over time markedly deviated from D^2 law. During the initial period, the curves of droplet squared diameter dropped at a faster rate whilst there existed a turning point, after which the slope of the curves became similar to the non-radiation curves. In other words, there seemed to be a critical diameter, below which the radiation absorption can be neglected. The major reason was that the importance of the radiation absorption on the droplet vaporization was strongly dependent on the droplet volume. The larger the droplet, the more significant role the radiation absorption would play in the evaporation process. Similar phenomena were reported elsewhere in the study of Long et al. [26]

Another reason for the varying slope found in the radiation curve lied in the fact that different components have different index of absorption. The continuously changing composition within the droplet were bound to vary the overall absorption energy and thus the overall evaporation rate [41]. In this case, the index of absorption of *n*-decane is much bigger than the index of absorption of toluene and butanol, because the *n*-decane molecules have much higher number of C-H bond than toluene and butanol. Apart from the discrepancy between the index of absorption of different component, the absorption of thermal radiation is inhomogeneous inside the droplet. It was reported that an enhanced radiation absorption was predicted for the central region of the droplet ($r < 0.65rd$). The spatial distribution of radiative absorption across the droplet diameter further complicated the evaporation process which contributed to the varying slopes of the radiation curves.

Comparison between low temperature and high temperature curves indicated that gas temperature was another key factor influencing the radiation absorption and hence the overall evaporation rate of the droplet. It can be seen from Fig. 6(a) and (b) that

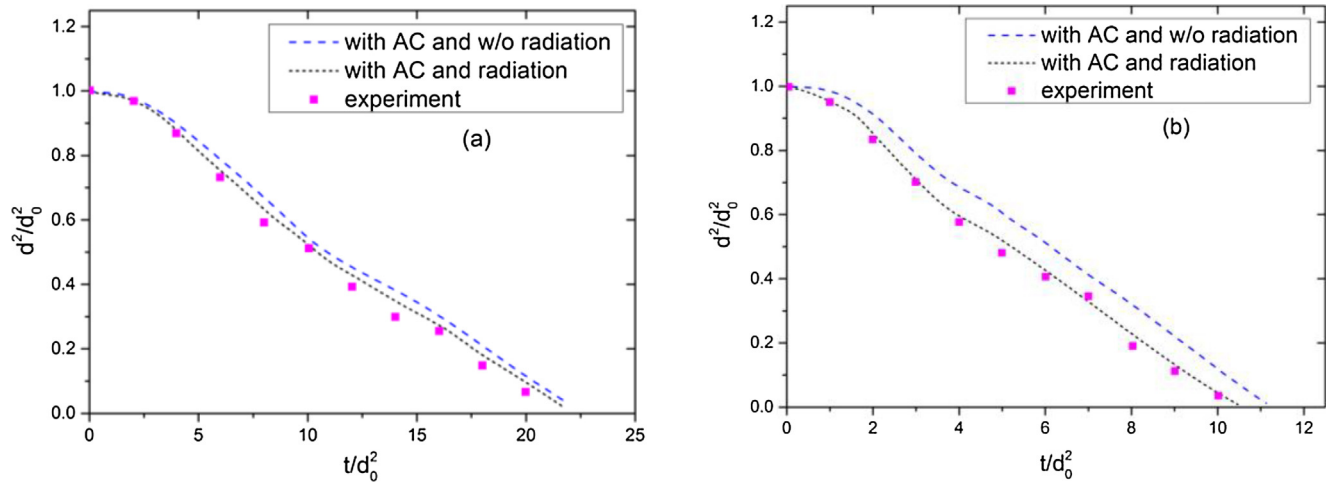

Fig. 6. Squared diameter versus time for droplets of 80% vol. *n*-decane, 15% vol. toluene, and 5% vol. butanol at two different gas temperatures (a) 503 K, (b) 703 K and predicted results with and without considering radiation.

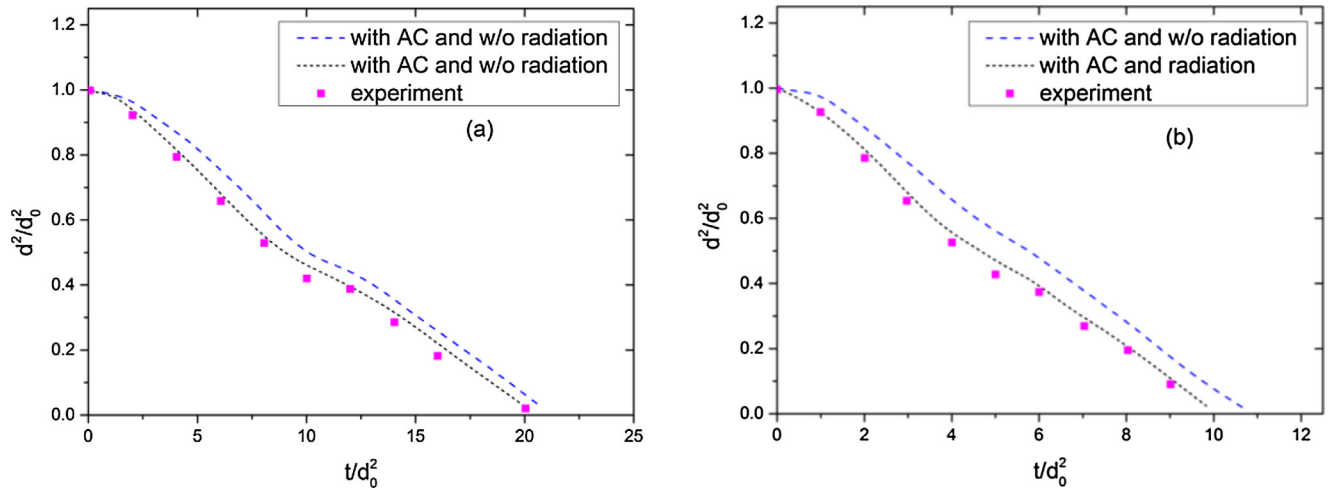

Fig. 7. Squared diameter versus time for droplets of 70% vol. *n*-decane, 15% vol. toluene, and 15% vol. butanol at two different gas temperatures (a) 503 K, (b) 703 K and predicted results with and without considering radiation.

when the gas temperature increased from 503 K to 703 K, the droplet lifetime reduced by 48% (from 22 s to 10.5 s). In addition, thermal radiation was insignificant at 503 K, but it was of great significance when the temperature increased to 703 K. At 503 K, the droplet lifetime of the cases with and without considering radiation were nearly the same. But for the temperature of 703 K, it clearly showed that the droplet lifetime of the cases with considering radiation reduced by about 10% compared with the cases without considering radiation. This was because that the higher the gas temperature, the bigger the Planck function in Eq. (15) and the more heat the droplet absorbed.

3.3. Concentration distribution inside droplets

Figs. 8 and 9 show the simulated results of concentration distribution inside the two test droplets by the model with considering activity coefficients and radiation. In general, the concentration of the component with small activity coefficient inside the droplet increased over time. This was due to the fact that the component with small activity coefficient evaporated slower than the component with large activity coefficient. For the concentration distribution at 10% droplet lifetime (DL), it can be clearly found that there was a turning point which was at the position of about 60% radius at 503 K and at the position of about 70% radius at 703 K. The liquid mass diffusion rate was less than the evaporation rate of the droplets, which resulted in different component concentration gradient between the region near the center and the region near droplet surface. The droplet was relatively big in the initial period of the evaporation, and the liquid in the center region was more difficult to diffuse to the surface region due to the longer distance, which further intensified the concentration gradient.

With time elapsed, more liquid components in the central region diffused to the surface region, thus the concentration gradient gradually decreased over time. Comparing with the initial period of the evaporation, there was no obvious turning point and the curve of concentration distribution within droplet was nearly flat. In other words, the influence of activity coefficient shrunk over time. This can be explained by analyzing the change of composition within droplet. As the evaporation progressed, the concentration of the components with large activity coefficients in the droplet were significantly reduced due to its high evaporation rate. Thus the overall evaporation process of the droplet approached the single-component evaporation process with small activity coefficient. In addition, droplet diameter reduced over time, thus the

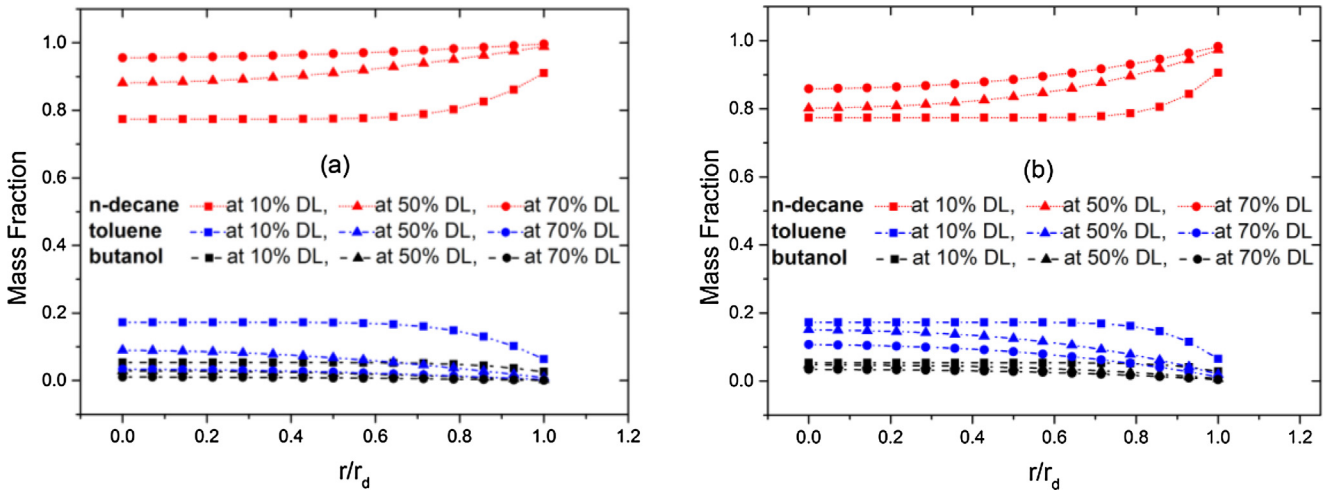

Fig. 8. Simulated concentration distribution inside the droplet of 80% vol. *n*-decane, 15% vol. toluene and 5% vol. butanol with considering activity coefficients and radiation at two different gas temperatures (a) 503 K and (b) 703 K.

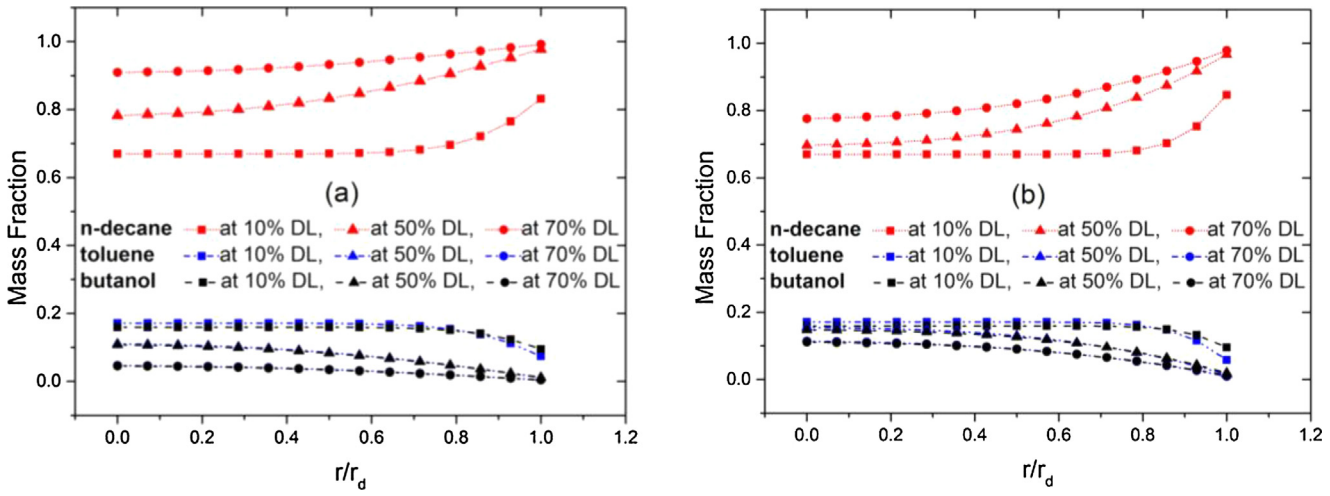

Fig. 9. Simulated concentration distribution inside the droplet of 70% vol. *n*-decane, 15% vol. toluene and 15% vol. butanol with considering activity coefficients and radiation at two different gas temperatures (a) 503 K and (b) 703 K.

mass diffusion would be enhanced due to the shortened transport distance from the central region to droplet surface. Therefore, the diffusion of the component with large activity coefficients from the central droplet could compensate the mass loss at surface via evaporation, which further decreased the concentration gradient.

The predicted temperature distribution profiles were not presented here because they turned out to be almost flat compared with the aforementioned component concentration distributions. This was attributed to the fact that thermal diffusivity in the liquid phase (in the order of 10^{-7}) is much larger than mass diffusivity (in the order of 10^{-9}) [42]. Therefore, any temperature gradients would reduce much faster than component mass gradients within the droplet.

4. Conclusion

An evaporation model incorporating component activity coefficient and external thermal radiation was developed to simulate multi-component non-ideal droplet evaporation process. Two test fuel droplets were used, which were mixtures of *n*-decane, toluene and butanol in different blending ratios. Suspended droplet experiments at different gas temperatures were conducted to compare against the simulated results. Both activity coefficient and radiation could enhance the predictive accuracy but their effects could be insignificant under certain conditions. Activity coefficient turned out to be insignificant at high temperature except for the ideal solutions. For non-ideal fuel droplets, there existed a turning point in the curve of the squared diameter over time in the evaporation process. The turning point appeared when the component with high activity coefficient nearly vanished via evaporation. For the droplet with a certain initial diameter, external radiation was significant at high temperature but not at low temperature. There was also a turning point in terms of droplet diameter after which the radiation became insignificant. The simulated results using the proposed model incorporating both non-ideality and radiation revealed that the uneven component distributions inside droplets changed significantly over time with different components exhibiting distinct trends.

Conflict of interest statement

We declare that we have no financial and personal relationships with other people or organizations that can inappropriately influence our work, there is no professional or other personal interest of any nature or kind in any product, service and/or company that could be construed as influencing the position presented in, or the review of, the manuscript entitled.

Acknowledgement

This research is supported by National Natural Science Foundation of China (91641119).

References

[1] H.R. Wang, J. Jin, J.B. Wang, N.X. Tan, L.I. Xiang-Yuan, Combustion mechanism of n-decane at high temperatures and kinetic modeling of ignition delay for aviation kerosene, Chem. J. Chin. Univ. 33 (2) (2012) 341–345.
[2] W.A. Sirignano, Fuel droplet vaporization and spray combustion theory, Prog. Energy Combust. Sci. 9 (4) (1983) 291–322.
[3] C.K. Law, Multicomponent droplet combustion with rapid internal mixing, Combust. Flame 26 (76) (1976) 219–233.
[4] R.B. Landis, A.F. Mills, Effects of internal resistance on the vaporization of binary droplets, 5th Int. Proceedings of the Heat Transfer Conf, Tokyo, Japan, 1974, Paper B7-9.
[5] C.M. Megaridis, Liquid-phase variable property effects in multicomponent droplet convective evaporation, Combust. Sci. Technol. 92 (4–6) (1993) 291–311.
[6] G.H. Hudson, J.C. McCoubrey, Intermolecular forces between unlike molecules. A more complete form of the combining rules, Trans. Faraday Soc. 56 (1960) 761–766.
[7] R. Hernández-Montelongo, J.P. García-Sandoval, E. Aguilar-Garnica, On the non-ideal behavior of the homogeneous esterification reaction: a kinetic model based on activity coefficients, Reaction Kinet. Mech. Catal. 115 (2) (2015) 401–419.
[8] S.W. Rick, S.J. Stuart, B.J. Berne, Dynamical fluctuating charge force fields: application to liquid water, J. Chem. Phys. 101 (7) (1994) 6141–6156.
[9] L. Chen, Z. Liu, Y. Lin, Z. Chi, Different spray droplet evaporation models for non-ideal multi-component fuels with experimental validation, Int. J. Heat Mass Transf. 94 (2016) 292–300.
[10] J. Camm, R. Stone, M. Davy, D. Richardson, The effect of non-ideal vapour-liquid equilibrium and non-ideal liquid diffusion on multi-component droplet evaporation for gasoline direct injection engines, SAE Tech. Pap. 2015 (3) (2015) 783–792.
[11] X. Ma, F. Zhang, K. Han, G. Song, Numerical modeling of acetone–butanol–ethanol and diesel blends droplet evaporation process, Fuel 174 (2016) 206–215.
[12] A. Fredenslund, R.L. Jones, J.M. Prausnitz, Group-contribution estimation of activity coefficients in nonideal liquid mixtures, AICHE J. 21 (6) (2010) 1086–1099.
[13] A. Bader, P. Keller, C. Hasse, The influence of non-ideal vapor–liquid equilibrium on the evaporation of ethanol/iso-octane droplets, Int. J. Heat Mass Transf. 64 (5) (2013) 547–558.
[14] S.S. Sazhin, A. Elwardany, P.A. Krutitskii, G. Castanet, F. Lemoine, E.M. Sazhina, M.R. Heikal, A simplified model for bi-component droplet heating and evaporation, Int. J. Heat Mass Transf. 53 (21) (2010) 4495–4505.
[15] S.S. Sazhin, A.E. Elwardany, P.A. Krutitskii, V. Deprédurand, G. Castanet, F. Lemoine, E.M. Sazhina, M.R. Heikal, Multi-component droplet heating and evaporation: Numerical simulation versus experimental data, Int. J. Therm. Sci. 50 (7) (2011) 1164–1180.
[16] S.S. Sazhin, M.A. Qubeissi, R. Kolodnytska, A.E. Elwardany, R. Nasiri, M.R. Heikal, Modelling of biodiesel fuel droplet heating and evaporation, Fuel 154 (1) (2015) 308–318.
[17] G. Brenn, L.J. Deviprasath, F. Durst, C. Fink, Evaporation of acoustically levitated multi-component liquid droplets, Int. J. Heat Mass Transf. 50 (25) (2007) 5073–5086.
[18] N. Al-Esawi, M. Al Qubeissi, S.S. Sazhin, R. Whitaker, The impacts of the activity coefficient on heating and evaporation of ethanol/gasoline fuel blends, Int. Commun. Heat Mass Transf. (2018).
[19] W.L.H. Hallett, S. Beauchamp-Kiss, Evaporation of single droplets of ethanol–fuel oil mixtures, Fuel 89 (9) (2010) 2496–2504.
[20] A. Zuend, C. Marcolli, A.M. Booth, D.M. Lienhard, V. Soonsin, U.K. Krieger, D.O. Topping, G. McFiggans, T. Peter, J.H. Seinfeld, New and extended parameterization of the thermodynamic model AIOMFAC: calculation of activity coefficients for organic-inorganic mixtures containing carboxyl, hydroxyl, carbonyl, ether, ester, alkenyl, alkyl, and aromatic functional groups, Atmosp. Chem. Phys. 11 (2011) 9155–9206.
[21] S.S. Sazhin, Modelling of fuel droplet heating and evaporation: Recent results and unsolved problems, Fuel 196 (1) (2011) 69–101.
[22] B. Abramzon, S. Sazhin, Convective vaporization of a fuel droplet with thermal radiation absorption, Fuel 85 (1) (2006) 32–46.
[23] H. Wang, R.D. Reitz, M. Yao, Comparison of diesel combustion CFD models and evaluation of the effects of model constants, SAE Tech. Pap. (2012).
[24] L. Dombrovsky, S. Sazhin, Absorption of thermal radiation in a semi-transparent spherical droplet: a simplified model, Int. J. Heat Fluid Flow 24 (6) (2003) 919–927.
[25] L.A. Dombrovsky, Thermal radiation from nonisothermal spherical particles of a semitransparent material, Int. J. Heat Mass Transf. 43 (9) (2000) 1661–1672.
[26] W. Long, P. Yi, M. Jia, L. Feng, J. Cui, An enhanced multi-component vaporization model for high temperature and pressure conditions, Int. J. Heat Mass Transf. 90 (2015) 857–871.
[27] D. Ju, J. Xiao, Z. Geng, Z. Huang, Effect of mass fractions on evaporation of a multi-component droplet at dimethyl ether (DME)/n-heptane-fueled engine conditions, Fuel 118 (1) (2014) 227–237.
[28] B.E. Poling, J.M. Prausnitz, J.P. O'Connell, The Properties of Gases and Liquids, fifth ed., 1987.
[29] B. Abramzon, W.A. Sirignano, Droplet vaporization model for spray combustion calculations, Int. J. Heat Mass Transf. 32 (9) (2013) 1605–1618.
[30] P.B. Govindaraju, M. Ihme, Group contribution method for multicomponent evaporation with application to transportation fuels, Int. J. Heat Mass Transf. 102 (2016) 833–845.
[31] J. Camm, R. Stone, M. Davy, D. Richardson, The effect of non-ideal vapour-liquid equilibrium and non-ideal liquid diffusion on multi-component droplet evaporation for gasoline direct injection engines, SAE Int. (2015).
[32] S.S. Sazhin, W.A. Abdelghaffar, P.A. Krutitskii, E.M. Sazhina, M.R. Heikal, New approaches to numerical modelling of droplet transient heating and evaporation, Int. J. Heat Mass Transf. 48 (19–20) (2005) 4215–4228.
[33] A. Tuntomo, C.L. Tien, S.H. Park, Optical constants of liquid hydrocarbon fuels, Combust. Sci. Technol. 84 (1) (1992) 133–140.
[34] P.P. Sethna, D. Williams, Optical constants of alcohols in the infrared, J. Phys. Chem. 83 (3) (1979) 405–409.
[35] C. Dale Keefe, S.M. Innis, Temperature dependence of the optical properties of liquid toluene between 4000 and 400 cmK1 from 30 to 105 8 °C, J. Mol. Struct. 737 (2005) 207–219.

[36] G.A.E. Godsave, Studies of the combustion of drops in a fuel spray—the burning of single drops of fuel, Symp. Combust. 4 (1) (1953) 818–830.
[37] X.Q. Chen, P.J.C. F, Numerical prediction of nonevaporating and evaporating fuel sprays under nonreactive conditions, Atomiz. Sprays 2 (4) (1992).
[38] I. Gökalp, C. Chauveau, H. Berrekam, N.A. Ramos-Arroyo, Vaporization of miscible binary fuel droplets under laminar and turbulent convective conditions, Atomiz. Sprays 4 (6) (1994) 661–676.
[39] T.T.B. Nguyen, S. Mitra, M.J. Sathe, V. Pareek, J.B. Joshi, G.M. Evans, Evaporation of a suspended binary mixture droplet in a heated flowing gas stream, Exp. Therm Fluid Sci. 91 (2018).
[40] N. Al-Esawi, A. Mansour, S Sergei Qubeissi, N. Sazhin, V Mike Emekwuru, Blundell, Impact of corrected activity coefficient on the estimated droplet heating and evaporation, International Conference on Thermal Engineering: Theory and Applications, 2018.
[41] A. Tuntomo, Transport phenomena in a small particle with internal radiant absorption (1990).
[42] L. Liu, Y. Liu, M. Mi, Z. Wang, L. Jiang, Evaporation of a bicomponent droplet during depressurization, Int. J. Heat Mass Transf. 100 (2016) 615–626.